



ASSESSMENT OF SSI EFFECTS ON A SEISMICALLY ISOLATED MULTI-SPAN BRIDGE UNDER BI-DIRECTIONAL SEISMIC EXCITATION

Alper Ucak¹, George Mavroeidis², Gokhan Pekcan³, Panos Tsopelas⁴

ABSTRACT

Elevated highway bridges are important elements in modern society infrastructure. Due to their strategic importance, loss of functionality in an earthquake is not an acceptable performance criterion. Observed performance of highway bridges following recent earthquakes suggested that conventional design methods might not provide the desired performance levels. Seismic isolation is an efficient alternative for mitigating earthquake effects for bridges. Recent seismic events have shown that if not designed properly, seismically isolated bridges that are thought to be safe may suffer severe damage (e.g. Bolu Viaduct, in Duzce Earthquake 1998) if not total collapse. Extensive research has been carried out in the past 30 years regarding the effects of soil structure interaction (SSI) on the seismic response of civil engineering structures and until recently it was believed that neglecting SSI effects would lead to a safe and conservative design. Case studies conducted after the Kobe (1995) earthquake reveal that for non-isolated bridges, SSI will affect the dynamic properties of the structure that in turn may be beneficial or in many cases detrimental to their seismic response. Herein the effect of SSI on the seismic response of a seismically-isolated bridge, Bolu Viaduct, founded on soft non-liquefiable soil is investigated. Accounting for the non-linear behavior of the seismic isolation system, the inertial interaction between the deep foundation and the superstructure is studied. It is shown that for certain conditions this interaction might increase the displacement demands imposed on the structure, which in turn might lead to loss of functionality of the structure. The results show that SSI is an important factor in the earthquake response of seismically isolated bridges and that these effects need to be considered in the design and detailing of the isolation system as well as in the evaluation of the overall performance of the structural systems during an earthquake event.

DESCRIPTION OF THE BRIDGE MODEL

The structure under consideration, Bolu Viaduct 1 is located in central Turkey and is a small but very important segment of the Trans-European Motorway, connecting Turkey's capital Ankara to Istanbul. The 2.3 km long viaduct consists of 59 dual spans, each being approximately 40 m long. The original design of the superstructure called for seven lines of simply supported pre-stressed concrete box girders for each span and a slab that was continuous over a segment of 10 spans (Figure 1). Each segment consists of 11 hollow core concrete piers with varying heights and a plan dimension of 4.5x8 m, resting on a massive 3 m thick pile cap (Roussis et al. 2003).

The foundation system of each pier consists of a 4x3 pile group consisting of 1.8m diameter cast-in-drilled-hole piles that pass tough soil with variable strength. However, due to the length of the structure and the presence of the Anatolian fault, precise characterization of the soil conditions along the viaduct is rather difficult. To the authors' knowledge, no (published) experimental data exists regarding mechanical properties of the soil, except the geotechnical profile and the trial pile test results, presented by Pane (2001) and Pane and

1 Post Doctoral Research Associate, The Catholic University of America, Washington, DC 20064

2 Assistant Professor, The Catholic University of America, Washington, DC 20064

3 Assistant Professor, University of Nevada Reno, Reno, NV 89557

4 Associate Professor, University of Thessaly, Volos, GR 38334, Greece

Barluzzi (1994). The geotechnical profile along a 300m length of the viaduct (which is approximately equal to the length of one segment of the structure) is reproduced from Pane and Barluzzi (1994) and presented in Figure 1.

In the original design a seismic isolation system consisted of lubricated flat sliders together with steel yielding devices. The isolation system and the viaduct were severely damaged during the 1999 Duzce earthquake due to inadequate size of the steel yielding devices (Roussis et al. 2003). After the earthquake the structure was retrofitted such that the superstructure (box girders and deck slab) was made continuous over the 10 span segment and each pier top was equipped with two large capacity friction pendulum bearings (FPS) (Priesly and Calvi 2002, Uckan 2007). Typical cross-section of the retrofitted pier along with the force deformation relationship of the FPS bearing is given in Figure 2.

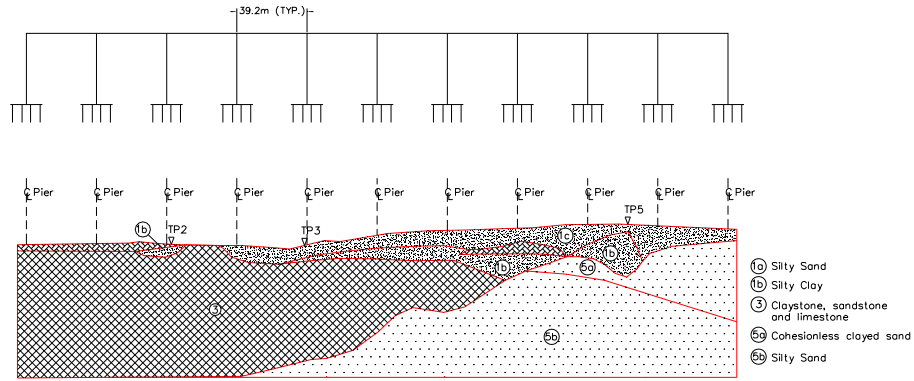


Figure 1. Elevation of one segment of the viaduct and the geotechnical profile

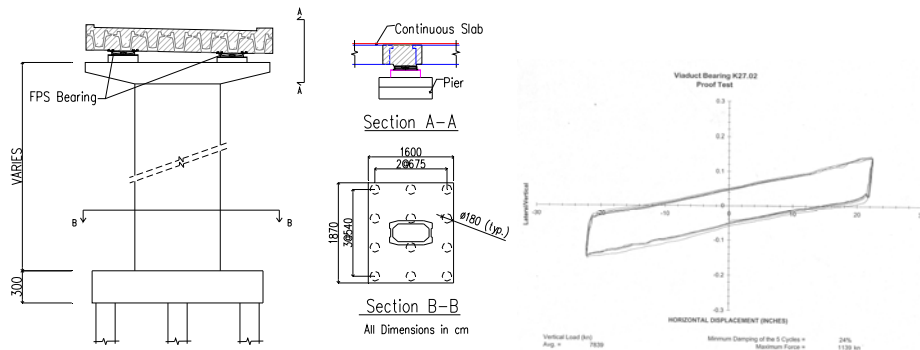


Figure 2. Typical cross-section of the pier and the experimental force deformation loops of the FPS (Uckan 2007)

DYNAMIC STIFFNESS OF PILE FOUNDATION

The dynamic impedance of a single pile can be expressed as:

$$\mathfrak{K}_j^S = K_j^S + i\omega C_j^S \quad (1)$$

where, the subscript j denotes the direction of the frequency dependent spring, i.e. x for horizontal, z for axial, r for rocking, K_j^S is the real part of the dynamic stiffness, C_j^S is the dashpot coefficient, and ω is the vibration frequency. The real part of Equation 1 can be re-written as:

$$K_j^S = K_j k_j \quad (2)$$

where, K_j is the static stiffness of the pile, k_j is the dynamic stiffness coefficient. The imaginary part of equation 1 on the other hand, can be evaluated using closed formed solutions available in the literature or using the integral expressing given in Gazetas and Dobry (1984)

$$C_j^S = \int_0^L c_j(\omega) Y_{sj}^2(z) dz \quad (3)$$

where, $c_j(\omega)$ is the distributed damping coefficient that accounts for both radiation and soil inherent damping, $Y_{sj}(z)$ is the static deflection profile of the pile normalized to its maximum amplitude on the top.

In this study the static stiffness (K_j in Equation 1) values of the piles are evaluated using the trial pile tests results, conducted at the viaduct site (Pane and Barluzzi 1994, and Pane 2001). The static deflection profiles on the other hand are determined using closed formed solutions of a beam-on-Winkler foundation model with an equivalent constant sub-grade reaction along its depth, which is back calculated from trial pile tests. For more information on beam-on-Winkler foundation model the interested reader is referred to Poulos and Davis (1980). The dynamic stiffness and the distributed damping coefficients are evaluated using the closed form equations given in Gazetas et al. (1992).

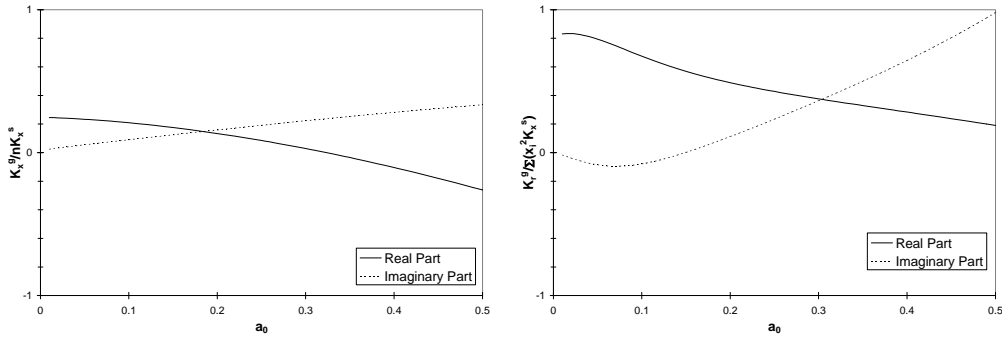


Figure 3 Lateral and rocking impedances of the 4x3 pile group used for pier foundation in Bolu Viaduct ($E_p/E_s=75$).

Once the impedance of a single pile is calculated the pile group impedance (of the 4x3 pile group) can be evaluated by applying the simplified super position method proposed by Dobry and Gazetas (1988).

Figure 3 presents the group stiffness and dashpot values for lateral and rocking motions, normalized with the sum of the static stiffness of the individual piles as a function of dimensionless wave parameter a_0 ($=\omega d/V_s$), with d being the pile diameter and V_s the shear wave velocity of the soil. The group impedance functions presented in the above figure are evaluated assuming linear-elastic soil and pile behavior and that no slippage or discontinuity occurs between the pile and the surrounding soil. In Figure 3 the stiffness at zero frequency ($a_0=0$) corresponds to the well-known static group efficiency factor, which could alternatively be determined using ‘p-y’ curves. The significance of pile-to-pile interaction is apparent from Figure 3, since the static group stiffness values are below unity. Furthermore the same figure shows the frequency dependency of the group dynamic stiffness values except the lateral dashpot coefficient that is constant over a wide range of frequencies.

While in a frequency domain analyses one could directly account for the frequency dependency of foundation springs and dashpots, the non-linear behavior of the isolation system requires a time domain solution that in turn makes it impossible to account for the frequency dependence foundation impedance functions. Moreover, with the isolation period

being fairly large it is expected that the isolated bridge will be excited by low frequencies that correspond to dimensionless wave parameter less than 0.05. For this reason the spring constants for the foundation system are assumed to be frequency independent and are evaluated at $a_0 \sim 0$. Although the horizontal dashpot coefficient is constant over a wide frequency range, the rocking dashpot coefficient shows some fluctuations at low frequencies. While this fluctuation constitutes a problem in selecting dashpot coefficient, parametric studies conducted by Ucak and Tsopelas (2007) using an asymptotic approach shows that rocking damping has no effect on the response of a structure with elasto-plastic isolation system. Based on those results rocking damping is ignored in the present analyses. Two sets of spring constants are used in the study, namely 'Case A' and 'Case B'. As can be seen from Figure 1 even for a single segment of the viaduct, the soil profile on which every pier is founded is quite different. This difference is accounted for in the spring values for set 'Case B'. In the set 'Case A' on the other hand the soil profile along the segment is assumed to be constant and the foundation springs are assumed to be equal to the lowest foundation spring value calculated in 'Case B'. The final values for the foundation springs are given in Table 1.

Table 1. Values for the foundation spring utilized in the present study

Pier #	Case A			Case B		
	K_x (GN/m)	C_x (GN·s/m)	K_r (GN·m/rad)	K_x (MN/m)	C_x (MN·s/m)	K_r (MN·m/rad)
P0,P1,P2				13.2	0.396	1220
P3,P4,P5,P6	5.4	0.162	395	7.8	0.234	610
P7,P8,P9,P10				5.4	0.162	395

SEISMIC EXCITATION

A total of 10 sets of accelerations time history pairs from 8 actual earthquakes are used in the present study. The seismic motions were chosen such that they will be representative of the motions that the considered bridge have or will experience. These events are mainly near fault records, however they have not been rotated to correspond to fault parallel and fault normal. The parenthesis next to the component label in Table 2 indicates the direction, longitudinal (L) or the transverse (T), of the bridge that the component was utilized in the analyses.

Table 2 List of the Seismic Excitations considered

RECORD ID	SEISMIC EVENT	STATION	COMPONENT
1	Duzce, Turkey, 1999	Duzce	DZC270(L) DZC180 (T)
2	Imperial Valley, California, 1979	El Centro Array #5	H-E05230(L) H-E05140(T)
3	Imperial Valley, California, 1979	El Centro Array #6	H-E06230(L) H-E06140(T)
4	Erzinca, Turkey 1992	Erzincan	ERZ-NS (L) ERZ-EW(T)
5	Hyogoken-Nanbu, Kobe Japan, 1995	KJMA	KJM090(L) KJM000(T)
6	Hyogoken-Nanbu, Kobe Japan, 1995	Takatori	TAK000(L) TAK090(T)
7	Tabas, Iran 1978	Tabas	TAB-TR(L) TAB-LN(T)
8	Northridge, California, 1994	Newhall	NWH360(L) NWH090(T)
9	Chi-Chi, Taiwan 1999	TCU 075	TCU075-W(L) TCU075-N(T)
10	Chi-Chi, Taiwan 1999	TCU 129	TCU129-W(L) TCU129-N(T)

ANALYSES AND DISCUSSION OF RESULTS

Viaduct Structural Model

A detailed model utilizing ANSYS (2004) software was built to carry out the analyses. This model is based on the model utilized by Roussis et al. (2003). The interested reader is referred to the Roussis et al. (2003) for details of the modeling parameters.

Modal and Harmonic Analyses

Eigenvalue and time-harmonic analyses were carried out to identify the differences in the dynamic characteristics between the fixed base structure and the one with foundation springs (Case B). In these analyses the isolation system is replaced with an elastic spring, with its stiffness equal to the post yielding stiffness of the FPS bearings. From the eigenvalue analyses the mode shapes of the first four modes, which correspond to the deck response, are shown in Figure 4. The longitudinal (1st mode), transverse (2nd mode), torsional (3rd mode) and transverse bending (4th mode) responses of the deck can be clearly identified. As can be seen from Figure 4 all the vibration modes associated with the deck (flexibility of the isolation system) show vibration periods in the range of ~5 secs (~0.2 Hz). The effect of SSI on the dynamic properties of the bridge manifested as period shift of the deck mode shapes is of the order of 0.01 Hz, which for all practical purposes is insignificant.

For the pier modes the picture is not as clear as for the deck. It is rather difficult to establish one to one correspondence between pier modes for the fixed base structure and the one with the foundation springs as can be seen in Figure 5, where modes 9th, 10th, 11th, and 12th are presented. This can be attributed to the complexity of the system and the fact that the two structures are different due to the presence of the foundation springs. To overcome this, time harmonic analysis was performed. In this analysis a harmonic force is applied at a particular location of the structure and the response at another location, as a function of frequency, is monitored. This analyses were performed with excitation applied and response monitored along both longitudinal and transverse directions of the structure. The harmonic force was applied at the center of the deck directly above pier No #6 and the displacement of pier No # 6 was monitored. The resulting displacement amplitudes as function of excitation frequency are depicted in Figures 6 and 7 for the longitudinal and the transverse directions of the bridge accordingly.

As can be seen from Figure6 the presence of the foundation springs resulted in a frequency shift along the longitudinal direction of 0.05 Hz (from 0.97 Hz fixed-base to 0.92 Hz with SSI springs). The frequency shift, 0.18 Hz (from 1.55 Hz fixed-base to 1.37 Hz with SSI springs), for the pier response along the transverse direction is 3.5 times larger than the shift observed along the longitudinal direction as shown in Figure 7. It should be noted that these frequency-shift values are for Pier #6 only because the response was monitored at that location. However, because the variations of the pier geometry for all the piers are not substantial and the distribution of the foundation-spring values is as shown in Table 1, it could be assumed, by exercising engineering judgment, that the frequency shifts of pier 6 are rather representative of the pier frequency shifts experienced by the structure as a whole along the longitudinal and transverse directions.

From the previous analyses, one could argue that since the deck mode frequency-shift (0.01 Hz), the pier frequency-shift along the longitudinal direction (0.05 Hz), as well as the pier frequency-shift along the transverse direction (0.18 Hz), are relatively small, the SSI effects on this particular structure must be negligible if non existent at all. This is the point which is attempted to be addressed in this paper through conducting non-linear time history analyses in the next section. In the mean time it is also constructive to look at the aforementioned frequency shift as changes of the fundamental periods of the structure as a

whole as follows:

- i) for the deck or isolation vibration mode the period change between the fixed-base structure and the structure with foundation springs is 0.4%,
- ii) for the longitudinal pier mode the period change is 5.4%, and
- iii) for the transverse pier mode the period change is 13%.

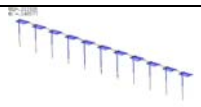
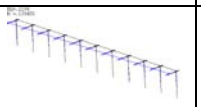
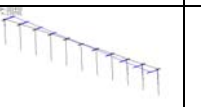
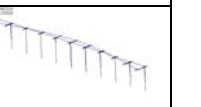
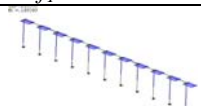
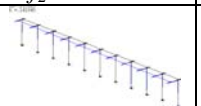


	<i>1st Mode</i>	<i>2nd Mode</i>	<i>3rd Mode</i>	<i>4th Mode</i>
<i>Fixed Base</i>				
	$f_1=0.211$ Hz	$f_2=0.219$ Hz	$f_3=0.221$ Hz	$f_4=0.445$ Hz
<i>Case B</i>				
	$f_1=0.210$ Hz	$f_2=0.218$ Hz	$f_3=0.220$ Hz	$f_4=0.444$ Hz

Figure 4. Mode shapes and frequencies of the first four deck modes of the Bolu Viaduct.

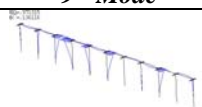
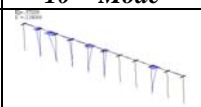


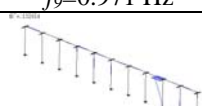
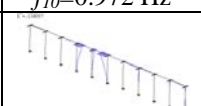


	<i>9th Mode</i>	<i>10th Mode</i>	<i>11th Mode</i>	<i>12th Mode</i>
<i>Fixed Base</i>				
	$f_9=0.971$ Hz	$f_{10}=0.972$ Hz	$f_{11}=0.972$ Hz	$f_{12}=0.972$ Hz
<i>Case B</i>				
	$f_9=0.902$ Hz	$f_{10}=0.924$ Hz	$f_{11}=0.925$ Hz	$f_{12}=0.925$ Hz

Figure 5. Mode shapes and frequencies of four pier modes of the Bolu Viaduct.

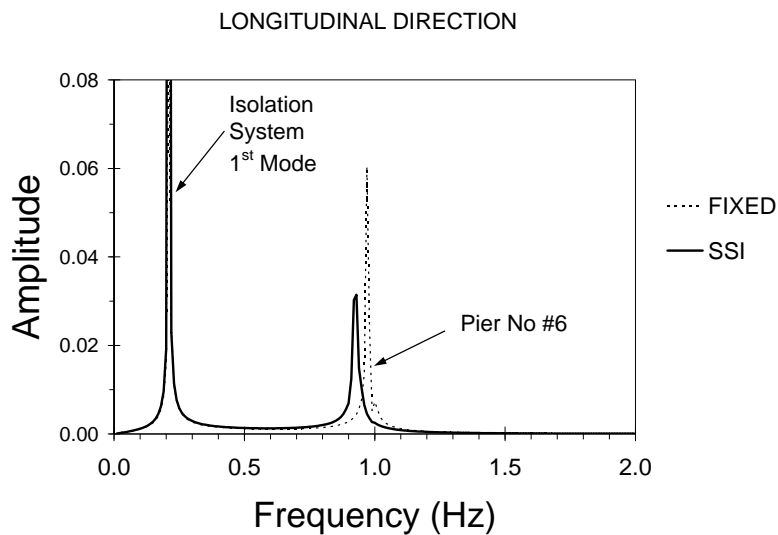


Figure 6. Pier #6 displacement vs frequency response along the longitudinal direction; for harmonic excitation on the deck along the longitudinal direction.

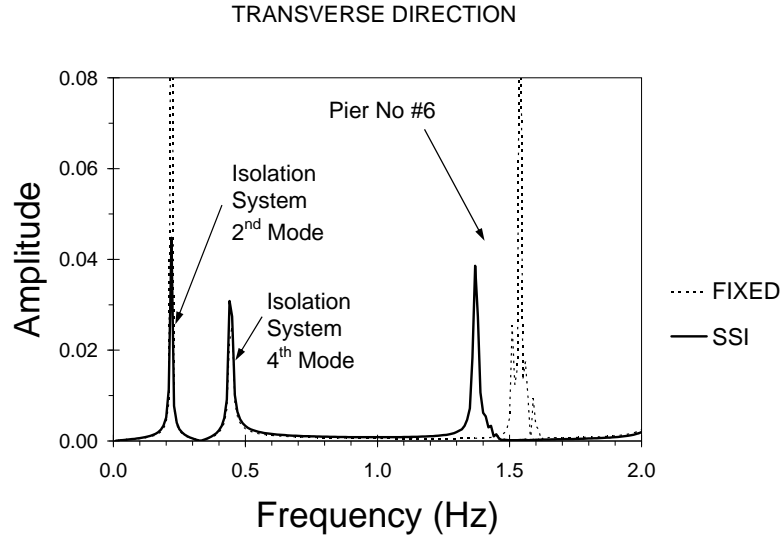


Figure 7. Pier #6 displacement vs frequency response along the transverse direction; for harmonic excitation on the deck along the transverse direction

Non Linear Time History Analyses

The isolated bridge system is analyzed using the set of 10 ground motion time histories shown in Table 1. The bridge is excited simultaneously in both longitudinal and transverse directions for the non-linear time history analyses. The choice of which seismic motion component will be used to excite which viaduct direction was made as follows: First the fixed pier viaduct was excited with the seismic motion component eg. A applied in the longitudinal direction of the bridge and the component B applied in the transverse direction of the bridge. Then a second analysis was performed with the seismic motion component B applied in the longitudinal direction of the bridge and the component A applied in the transverse direction. The peak values from these two analyses were recorded and the scenario which resulted in the largest response was chosen; thus assigning the components of each motion to a particular viaduct direction.

The system responses considered are the resultant displacement of the isolation system (isolation drift) at every pier location and the resultant shear force of every pier. The resultant values are calculated from the longitudinal and the transverse responses as the square root of the sum of the squares at every time instant. The peaks of the resultant values for the cases with the foundation springs (accounting for SSI) were normalized by their corresponding peaks of the resultant values obtained from the cases with fixed piers. The results, therefore, are presented in terms of resultant pier shear ratio (PSR) and resultant isolation drift ratio (IDR), which are defined as

$$Pier\ Shear\ Ratio = \frac{Pier\ Shear(V_s)}{Pier\ Shear(V_s = \infty)} \quad (4)$$

$$Isolation\ Drift\ Ratio = \frac{Isolation\ Drift(V_s)}{Isolation\ Drift(V_s = \infty)} \quad (5)$$

Figure 8 presets the resultant of the isolation drift ratio IDR with respect to the pier location occurring. It should be noted that the peak values used in calculating the IDR are maximum resultant values of isolation drifts which might not occur at the same time for the fixed-base structure and the structure with foundation springs. As can be seen from this figure, SSI clearly affects the maximum responses of the isolated bridge structure. The SSI effects seem to be either unfavorable or beneficial depending mainly on details of the

individual seismic records. Figure 8 show that when SSI effects are accounted for, the maximum resultant isolation drift has a spread ranging up to +14% relative to the fixed pier solution.

Figure 9 depicts the variability of the isolation system drift at every pier location for all motions. The maximum resultant isolation drift has a spread of ~1m ranging between 0.3 m and 1.3 m. It is interesting to note that the highest isolation drift demand ~1.3 m results for a case with foundation springs.

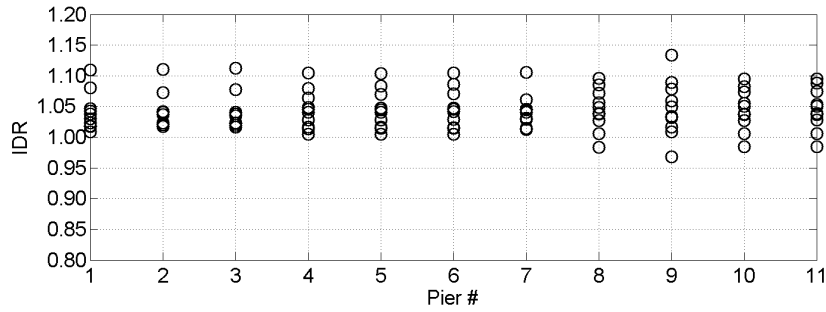


Figure 8 IDR vs Pier Number for all Motions

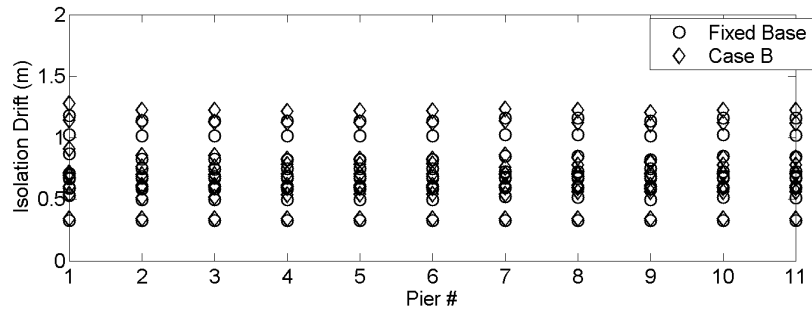


Figure 9 Variability of resultant Isolation Drift vs Pier Number for all Motions

Figure 10 summarizes the results obtained from non-linear time history analyses for the ground motion suite considered. The Record ID in Figure 10 corresponds to the Record ID numbers presented in Table 2. It should be noted that the peak values used in calculating the IDR and the PSR are maximum resultant values of isolation drifts and pier shears which might not occur for all seismic motions at the same location for the fixed-base structure and the structure with foundation springs. Again Figure 10 shows that SSI clearly affects the maximum responses of the isolated bridge structure in spite the fact that the SSI effects are favorable for some seismic motions and are unfavorable for others. This indicates that the details of individual seismic motions might contribute substantially on how SSI influences the response of the bridge. Figure 10 show that when SSI effects are accounted for, the maximum isolation drift has a spread ranging up to +12% relative to the fixed pier solution. While this increase might not seem important at first glance, for Record ID #3 this increase translates to approximately 120 mm. Realizing that the original isolation system (prior to retrofit) had an ultimate capacity of 480 mm, puts the importance of this increase into perspective. Similar observations can be made for the pier shear ratio, the spread relative to fixed pier solution is $\pm 10\%$, except for Record ID #7, which shows a 30% increase in pier shear ratio, a rather high change.

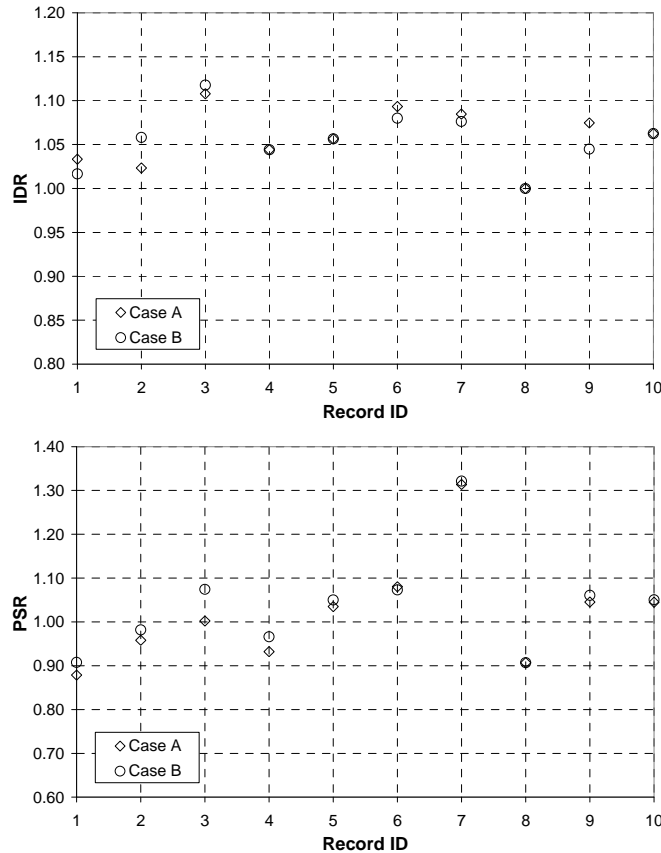


Figure 10 IDR and PSR vs Seismic Motion Number

CONCLUSIONS

The effects of SSI on the response of a seismic isolated bridge, the Bolu Viaduct, are investigated in this study. SSI is manifested through the flexibility of the foundation-soil system. The foundation considered consists of a 4x3 pile group. The premise that the SSI effects, since they increase the flexibility of the system and thus the isolation effect, are benefiting the seismic isolated bridges does not seem to hold true, as it is shown in Figure 8. The range of variation of the isolation drift and the pier shear as compared to the same responses for the case of no SSI, fluctuates between +25% and -10%. This indicates that SSI effects could be either favourable or unfavourable on the response of the seismic isolated bridges. Even though such variations might not look spectacular, they are very large and could potentially lead in failures if the SSI effects are not accounted properly. The results were obtained using a suite of seismic motions, and thus the conclusions could be limited by this choice.

REFERENCES

- ANSYS Inc. (2004), ANSYS V8.1 Users Manual
- Dobry, R., Gazetas, G., (1988) "Simple method for dynamic stiffness and damping of floating pile groups" *Geotechnique*, 38(4), 557-574
- Gazetas, G., Dobry, R. (1984) "Horizontal response of piles in layered soil", *Journal of Geotechnical Engineering*, 110(1), 20-40
- Gazetas, G., Fan, L., Tazoh, T., Shimizu, K., Kavvadas M., Makris N., (1992) , "Siesmic pile-group-

- structure interaction”, Piles Under Dynamic Loads, E., Prakash, .(ed.), ASCE, 56-93...
- Pane, V., (2001). “The November 1999 Duzce earthquake: assessment of the foundation damage of Viaduct n.1. of the Anatolian Motorway”, Proc. 15th International Conference on Soil Mechanics and Geotechnical Engineering-TC4 Satellite conference on Lessons learned from recent strong earthquakes, Istanbul
- Pane, V., Barluzi, M., (1994). “Some remarks on the behavior of three large diameter bored piles”, In Pile foundations: experimental investigation, analysis and design; Proc., Int. Workshop, Napoli, CUEN
- Poulos, H.G., Davis, E.H, (1980) “Pile foundation analysis and design”, John Wiley and Sons, New York
- Priesly, M.J.N., Calvi, G.M., (2002). “Strategies for repair and seismic upgrading of Bolu Viaduct 1, Turkey”, Journal of Earthquake Engineering, 6(1), 157-184
- Roussis, P.C., Constantinou, M.C., Erdik, M., Durukal, E., Dicleli M. (2003). “Assessment of Performance of Seismic Isolation System of Bolu Viaduct.” Journal of Bridge Engineering, 8(4), pp.182-190
- Ucak, A., Tsopelas, P., (2007). “Response of seismic isolated bridges including soil structure interaction effects”, Proc., 4th International Conference on Earthquake and Geotechnical Engineering, Thessaloniki, 4ICEGE
- Uckan, E., (2007), Personal communication